Exploring sheath-core yarns technology to optimise bio-composite performances

Delphine Quereilhac, Jules Femery, Guillaume Morel, Adrian Korycki, Emmanuel de Luycker, Pierre Ouagne, France Chabert

Materials Research Proceedings 28 (2023) 1809-1818 https://doi.org/10.21741/9781644902479-196

Exploring sheath-core yarns technology to optimise bio-composite performances

QUEREILHAC Delphine[1,a *], FEMERY Jules[1,b], MOREL Guillaume[1,c], KORYCKI Adrian[1,d], DE LUYCKER Emmanuel[1,e], OUAGNE Pierre[1,f] and CHABERT France[1,g]

[1]Univ. de Toulouse, Laboratoire Génie de Production, LGP, INP-ENIT, F-65016 Tarbes, France

[a]delphine.quereilhac@enit.fr, [b]jfemery@enit.fr, [c]guillaume.morel@enit.fr, [d]adrian.korycki@enit.fr, [e]emmanuel.de-luycker@enit.fr, [f]pierre.ouagne@enit.fr, [g]france.chabert@enit.fr

Keywords: Flax, Biocomposite, Extrusion, Sheath-Core, 3D Printing

Abstract. This work focuses on the design and fabrication of a continuous filament made of flax yarn and bio-based thermoplastic polymer. For this purpose, the sheath-core process has been explored by using an extrusion laboratory line equipped with a wire coating die to manufacture a flax core coated with PLA. The polymer properties were investigated (thermal transition, mechanical properties, melt viscosity) to link the polymer properties, the process and the properties of the resulting filament. The filament diameter decreases and surface defects appear when the pulling speed increases. The mechanical characterization of flax/PLA filaments demonstrates a higher elastic modulus, higher stress at break and lower strain at break as compared with pure PLA filaments. Such PLA coated flax filaments are a relevant option to widespread the use of biobased composites.

Introduction

Generalities about biocomposites.

Working with eco-friendly materials, recycling, and reusing are key challenges to face the demand for renewable resources. According to this statement, biocomposites are a great attraction, as they are produced from biofibers and biopolymers, and can present the required properties and functionalities at a reasonable cost [1]. The biocomposites market forecast report has estimated that the market size is likely to attain $10.89 billion by 2024, and the fabrication of materials from biobased feedstock is likely to raise from 5% in 2004 to 18% in 2020, and ~25% in 2030 [2]. Vegetal fibers such as flax and hemp have attracted significant focus as a potential alternative to synthetic fibers like carbon and glass [3], and biocomposites have been largely employed for several secondary applications in aerospace, automotive, packaging, electronics, and building sectors. It is thus important to keep developing new processes to widen the application panel of these renewable materials.

The choice of reinforcement largely relies upon the inherent chemical and physical characteristics of the fibres. Right from the cultivation to processing phases, various factors such as environmental conditions, processing methods or fiber age, influence the properties of plant fiber. Some of these features also have a direct effect on several biocomposite responses such as fiber-matrix bonding, thermal stability, or moisture sensitivity [4]. On the other hand, considerable research works are being performed in developing fully biodegradable materials (green composites) by combining biodegradable polymer matrix with biofiber [5]. The manufacturing of natural fibre-reinforced biocomposites is based, in general, on the technologies used for conventional synthetic short fibre composites, such as extrusion, injection moulding or compression moulding. Nevertheless, suitable processing methods and conditions must be chosen to manufacture fibre-reinforced biocomposites. To obtain biocomposites with suitable properties,

it is crucial to control their thermal stability, interfacial adhesion, fiber distribution, type and content [6].

Flax fibres.

In this work, flax has been chosen among all vegetal fibres for its good mechanical properties and its availability at industrial level and local scale. After extraction from the flax straw (woody core), fibres are organised in bundles, linked by a middle lamella, which cements the cell walls of adjacent cells together. It is mainly composed of pectic polysaccharides, lignin, and a small amount of proteins [7]. Many industrial processes aim to remove this natural matrix, to improve the separation of elementary fibres and the composite matrix/flax adhesion. However, these processes also bring undesirable side effects such as deterioration of the fibre and loss of mechanical performance [8].

Sheath-core flax/PLA.

Nowadays, flax is often found in composite materials under the form of unidirectional ply, woven, or short fibres, but an emerging technique is the use of long fibres for 3D printed composites. Material extrusion is defined as an additive manufacturing process in which material is selectively dispensed through a nozzle. Additive manufacturing process creates complex 3D parts through directionally orientated extrusion. The simplicity and relatively low price make of material extrusion make it widely used in many research works [9]. Two main options exist to print composites with continuous natural fibres: (i) in-nozzle impregnation in which the yarn and the molten matrix arrive simultaneously inside the noozle, and (ii) pre-impregnated filament printing in which the core yarn is trapped into a matrix sheath. Simultaneous impregnation of thermoset resin and continuous fibre in the extrusion head leads to several process issues, such as fibre content and feed, deposition rate and path [9]. Also, passing fibre and thermoplastic filament through a single nozzle limits control over fibre and can lead to poor overall surface finish and increased voids [10].

In this work, a novel process will be explored to improve the quality of a sheath-core filament, made of flax yarn coated by a PLA (polylactic acid) matrix. PLA is a bio-based polymer which uses have been drastically widen these last years, as it is renewable and biodegradable, and it is obtained from agricultural crops like sugar beet or corn. It demonstrates good mechanical strength, stiffness and can be processed with conventional polymer processing techniques. In addition, when looking at its life cycle, it appears that PLA requires nearly one tenth of the fossil energy when compared to synthetic polymers [11]. These factors make PLA an ideal choice to experiment biodegradable composites. In this research work, material intrinsic parameters were explored such as fibre properties, PLA thermal transitions and melt viscosity. Then, several filaments were manufactured with a wire coating die equipment while varying the pulling speed. Then, the structure and the properties of the resulting filaments were investigated to correlate the PLA properties with mechanical behaviour of the filaments.

Materials and Methods

Flax yarn.

The first test batch was carried out on flax sliver, which is a product originally manufactured for garment-textile fabrication. In order to design a very thin and soft yarn, this flax material has been prepared for wet spinning process: firstly, the fibres have undergone a chemical degumming process with low concentration caustic soda. This step is crucial to separate cellulose and non-cellulose parts and to get rid of all the pectins and sticking agents present on the fibres to keep their cohesion. Also, this process turns the flax from hydrophobic to hydrophilic, which is a major requirement for the wet spinning process. After degumming, fibres were bleached with peroxide to prepare them for further transformation and finishing, such as dyeing. Flax sliver was turned to yarn on a Linimpionti BMR1 wet spinning machine, presented in Fig. 1a. Machine speed was 15m.min^{-1}, with a drawing of 4, and a torsion of 450 revolution.min^{-1}. Final yarn has a count of 66

± 3 Tex. For flax yarn characterisation, the tensile tests are carried out on a Tenso-Lab 4 v. (Mesdan Lab, Italy) apparatus, according to standard NF EN ISO 2062 [12] over a length of 250 mm, with a speed of 250 mm.min^{-1} and a preload of 0.50 cN.Tex^{-1}.

PLA 3 grades.

PLA is a linear thermoplastic aliphatic polyester obtained from lactic acid. As shown in Fig. 1b, lactic acid has two enantiomer form L-Lactic and D-Lactic acid due to its chiral geometry. It results in dimers with three enantiomer forms: L-lactid, D-Lactid and DL-Lactid [13]. In this work, two different grades of PLA are studied from NaturePlast: PLE005 and PLE005-A (called respectively in this work PLA-A and PLA-B). PLE005 (PLA-A) is a homopolymer of L-lactid (>99%) with high crystallisation potential and PLE005-A (PLA-B) is a copolymer of L-Lactid (>95%) and D-Lactid (<5%) with slower crystallisation kinetics due to the presence of D-Lactid [14]. PLA pellets were systematically dried in an oven at 60°C for few hours before any experiment. Indeed, the presence of water in PLA while processing can affect its property by hydrolysis phenomenon and plasticising of the crystalline phase [15].

Extruder and wire coating die.

The wire coating die is presented in the scheme in Fig. 1c. The die is a commercial equipment provided to fit a single screw Rheomex extruder on a Polylab OS system by ThermoFisher. The flax fiber enters through the top and exits at the bottom of the scheme. The molten polymer enters at the left side and it flows into a tube up to join the fiber to coat it. The screw is L/D= 25 and its rotating speed is kept constant at 5 rpm. The temperatures are 180°C for the screw, 170°C inside the die. Then, the fiber coated with the molten PLA exits the die at the bottom of the scheme. The coated fiber is pulled out the die with a system equipped with 2 rollers. The pulling speed has been varied between 0.003 and 0.2 m.s^{-1}. The flow is considered as steady, incompressible and isothermal, the flowing profile is a Poiseuille-type, with a maximum fluid velocity ($V_{r=R}=V_{max}$) at the vicinity of the fiber and a sticking condition at the die wall ($V_{r=0} = 0$). A modular part can be changed to vary the thickness of the polymer coating, the nozzle dimensions chosen in this study are 2 and 4 mm. The maximum shear rate just before exiting the die $\dot{\gamma}$ is calculated by V_m/e, with e the width of the channel where the polymer flows. The maximum shear rate is 200 s^{-1} for a 2 mm diameter filament.

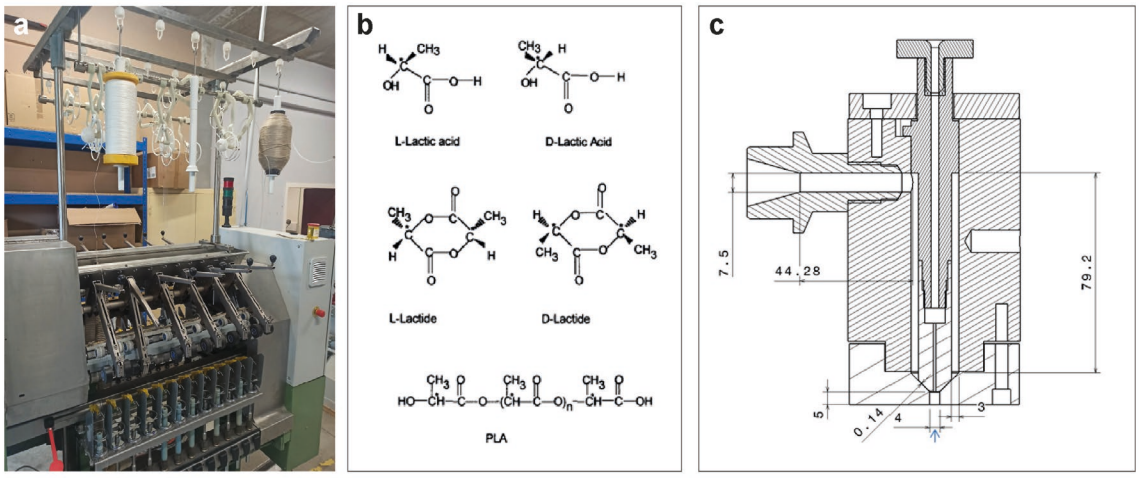

Fig. 1. Wet spinning machine (a), structures of lactic acid, lactid and PLA [15] (b), wire coating dye (c).

Rheological behavior.

The polymer coating thickness could be predicted by considering the process parameters and the polymer rheological properties. For that, we measured the complex viscosity of the two grades of PLA in an oscillatory rheometer MCR501 by Anton Paar, applying the Cox-Merz equivalence.

The experiments were carried out using a 25 mm diameter parallel-plate configuration with a 1 mm gap. Initially, dynamic strain sweeps were performed to determine the linear viscoelastic regime (LVR). Time sweeps were performed to check the thermal stability of the polymer along the experiment duration. Frequency sweeps were performed to measure G' and G'' between 200 and 230°C with 10°C steps, from 100 to 0.1 rad.s^{-1}. Since the angular frequency is limited to 100 rad.s^{-1}, we applied TTS at the reference temperature of 200°C to extend the shear rate range to attain the 200 s^{-1} involved in the process.

DSC.

The thermal transitions and enthalpy were determined using a Mettler Toledo DSC1 under a nitrogen flow rate of 50 mL.min^{-1}. After heating at 210°C to cancel the thermomechanical history, a cooling rate at 10°C.min^{-1} was applied followed by a second heating ramp at 10 °C.min^{-1}.

Mechanical characterisation.

For pure PLA, specimens were injected on a Proxima H120 (Billion, France) at 190°C to 175° from nozzle to rear barrel with mould regulated at 40°C to achieve a low crystallinity. The tensile tests were carried out on a 33R4204 (Instron, United State) testing machine, equipped with a mechanical extensometer 2620-604 (Instron, United State) and a load cell 2525-805 of 5kN (Instron, United State) according to standard NF EN ISO 527 with a speed of 3mm.min^{-1}. In this study, five specimens were tested for each grade of PLA.

Optical observations. A microcutting machine Mecatome T202 (PRESI, France) was used for sample preparation with an ultra-thin wheel UTW-R200U (PRESI, France). Samples were directly observed on their cross-sections with a binocular Leica Wild M420 at magnification of x40. The surfaces of PLA filaments were inspected through a high-resolution microscope Keyence VHX-6000S (Bois-Colombes, France) in a reflection and transmission mode with a magnification of x100.

Results

Mechanical characterization of PLA.

The tensile behaviour of both PLA is shown in Fig. 2. PLA-A and PLA-B show an elastic domain in their first percent of elongation indicating no modification in their microstructure. Then, PLA display a plastic domain where modifications in the microstructure appear, mainly chains' conformation and crystalline slip, until specimens breaking.

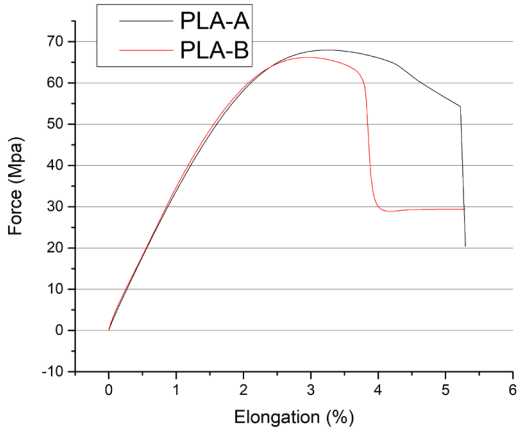

Fig. 2. Tensile curve of PLA-A and PLA-B.

The tensile properties of PLA-A and PLA-B are shown in Table 1. PLA-A, despite its low crystallinity due to high cooling rate during injection molding, has a slightly higher rigidity and strain at yield point than PLA-B. Previous studies have shown that a higher crystallinity of homopolymer of PLLA improves its rigidity and resilience [16]. PLA-B accepts longer elongation

before breaking than PLA-A because of less crystallinity resulting in higher macromolecular mobility.

Table 1. Mechanical properties of PLE005 and PLE005-A

	Young Modulus	**Stress at yield point**	**Elongation at yield point**	**Elongation at break**
	(Mpa)	(MPa)	(%)	(%)
PLA-A	3700	67.6	3.17	4.10
PLA-B	3500	65.2	3.08	>15

Thermal transitions of PLA.

Thermal transitions of PLA upon heating are shown in Fig. 3a. Glass transitions of PLA-A and PLA-B are 66°C and 60°C respectively. Their melting point are 178°C for PLA-A and 155°C for PLA-B. Those temperatures depend of the initial composition of PLA and its molecular weight. Also, the crystalline phase has stronger intermolecular interaction and lower flexibility [17], increasing the melting temperature. As expected, PLA-A reaches a higher crystallinity than PLA-B due to its higher concentration of L-Lactide. In Fig. 3b, DSC thermogram shows that PLA-A starts to crystalize at 117°C when cooling from a molten state. The crystallisation kinetics depends on its concentration of L-Lactid and molecular weight. At a cooling rate of 3°C.min^{-1}, PLA-B does not undergo crystallisation when cooling from a molten state due to presence of D-Lactid. Variation of D-Lactid concentration affects the crystallisation kinetics of PLA, at concentration higher of 15%, its crystallisation is not possible. Authors have shown that the crystallisation of PLA is 60 times faster from a concentration of 6.6% to 0.6% of D-Lactid [13].

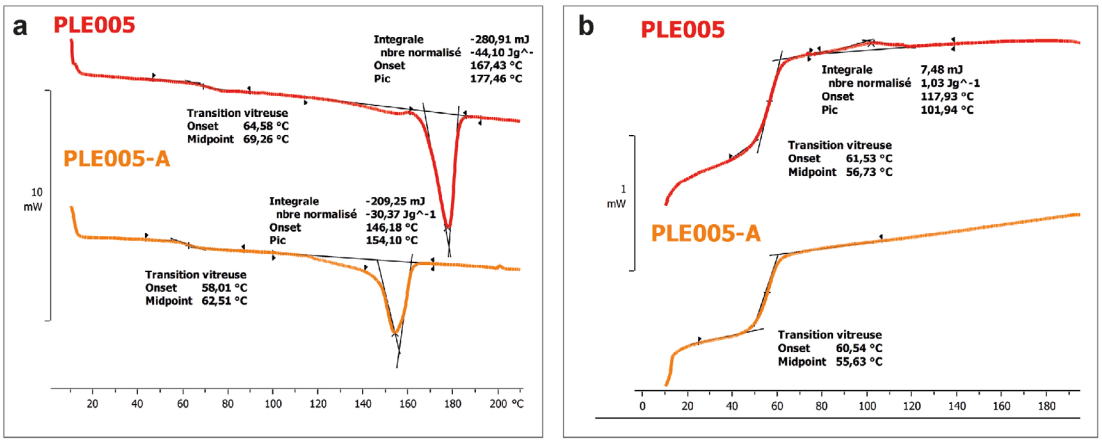

Fig. 3. DSC thermograms of PLA, heating ramp (a) cooling ramp (b).

Viscosity of PLA.

TTS was applied to frequency sweeps at 200, 210 and 220°C to obtain master curves shown in Fig. 4. The curves do not follow the rheological behavior expected for molten polymers, indicating a structural evolution with time. However, the slopes of G' and G'' are closed to the ω^1 and ω^2 dependency. This complex flowing behavior is mentionned in the literature: Lactic acid exists in two enantiomeric forms, L-lactic acid and D-lactic acid, whose co-crystallization forms a stereocomplex with a melting point about 50 °C higher than PLA homocrystals [18]. Neat PLLA demonstrates a Newtonian plateau at low frequencies, typical of polymer melts, while such

behavior is not observed when PLLA is blended with 5% PDLA. In the presence of PDLA, significant deviation of complex viscosity at low frequencies can be associated to the interaction between chains caused by stereocomplex formation [19]. This agrees with our findings, the master curve deviate from the expected trend for PLA-B which contain <5% of PDLA according to the manufacturer. Also, the complex viscosity of PLA- B is higher than those of PLA-A, likely due to the presence of a small concentration of stereocomplex in the PLLA melt. Moreover, measurement of the melt rheological properties of PLA is complicated by degradation effects resulting in chain breakage. Master curves of dynamic viscosity constructed using time-temperature superposition show significant dispersion for unstabilized PLA [20]. Finally, the complex viscosity of PLA-A and PLA-B is about 100 and 250 Pa.s respectively, at the Newtonian plateau.

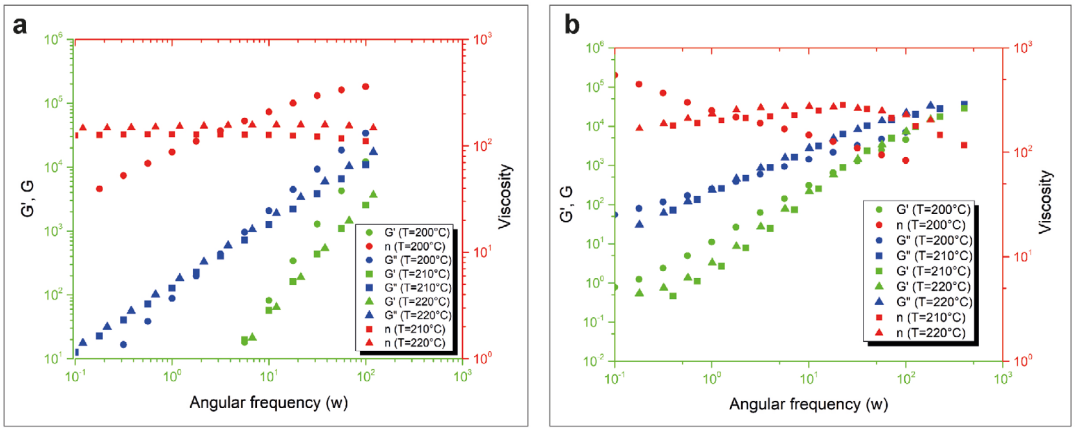

Fig. 4. Viscosity curves of PLA-A (a) and PLA-B (b).

Extrusion rates are often limited by the surface defects that appears at the die exit when the shear stress is too high [21]. At the die exit, the velocity profile goes from a parabolic shape to a plug one, resulting in tensile stresses that can crack the surface of the extrudate. This is known as the shark skin effect. In our cases, this defect is more likely to appear for PLA-B whose viscosity is higher, for the same shear rate, hereby related to the pulling speed. Such surface defects are seen in Fig 5 for both PLA. At low pulling speed, the filament surface of PLA-A is smooth Fig. 5a, whereas air bubbles Fig. 5b and shark skin effect Fig. 5c are visible for higher pulling speed. As expected, no shark skin effect was noticed for PLA-A due to a lower viscosity as seen in Fig. 4. Since PLA and flax fiber were thoroughly dried before processing, these bubbles could not stem from residual water. Another explaination could be associated with the design of the die in which the molten polymer could trap air where it meets the fiber.

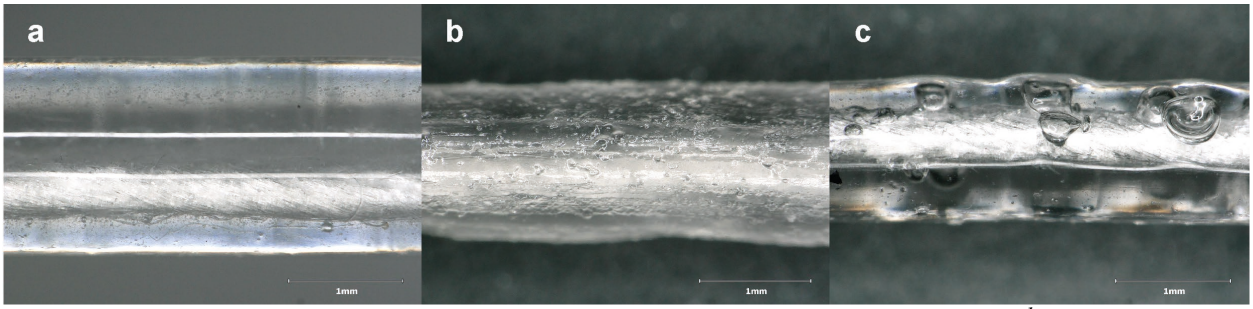

Fig. 5. Optical micrographs of PLA filament surfaces of PLA-A at 0.014 m.s^{-1} (a), PLA-A at 0.040 m.s^{-1} (b), PLA-B at 0.040 m.s^{-1} (c).

Microscopic observations of PLA injected with flax yarn.

Table 2 presents the longitudinal section of PLA extruded with flax yarn. Cross-sections show a clear irregularity in the location of the flax yarn: it tends to go to the side of the filament instead of its centre.

Table 2. Transversal section of the filaments, depending of the pulling speed and grade (PLA-A and PLA-B).

Pulling speed	PLA-A	PLA-B
0,008 $m.s^{-1}$	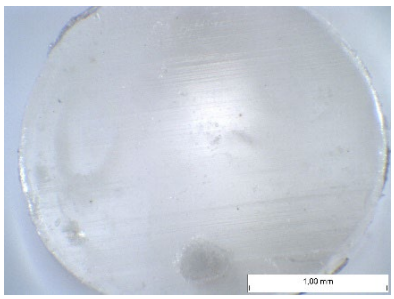	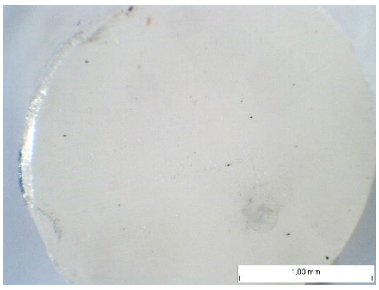
0,014 $m.s^{-1}$	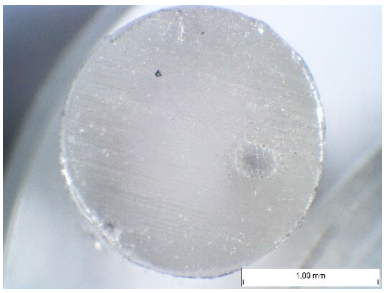	
0,040 $m.s^{-1}$	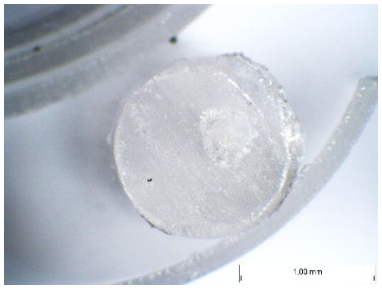	
0,065 $m.s^{-1}$		

Mechanical properties of PLA injected with flax yarn.

Fig. 6a shows the filament diameters for the two grades of PLA. As expected, when the pulling speed increases, the PLA coating thickness around the flax fibre get thinner. No effect of the viscosity is seen, since the diameters are similar for both grades Fig. 6b shows the impact of pulling speed on the stress strain curve of the two PLA/flax (PLA-A and PLA-B) filaments pulled at 0.008,

0.014, 0.040 and 0.065 $m.s^{-1}$. It appears that the highest is the shear rate, the lowest is the strength at break: a fast-pulling speed creates a thinner polymer layer onto the flax yarn.

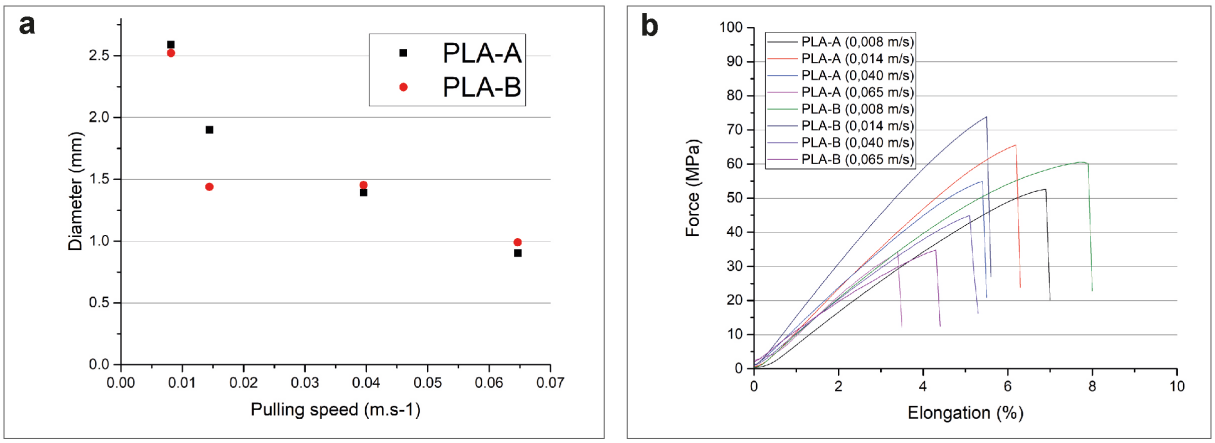

Fig. 6. Evolution of the diameter with the pulling speed (a), Stress strain curve of PLA-A and PLA-B for 4 pulling speed (b).

Fig. 7a presents the stress strain curve of flax yarn, pure PLA filaments and PLA coated flax filaments (referred as PLA injected). It is clear that adding flax yarn, which has naturally a higher stiffness, increases the filament rigidity and decreases the elongation at break compared to pure PLA filaments. The impact of PLA grade and pulling speed is less obvious. Fig. 7b presents the elastic modulus of pure PLA-A and PLA-B for the 4 pulling speed, along with PLA-A and PLA-B coated flax at one speed. The elastic modulus is higher for filaments containing flax. When increasing the pulling speed, the elastic modulus decreases. This could be attributed to the surface defects appearing at high shear rates as seen in Fig 5.

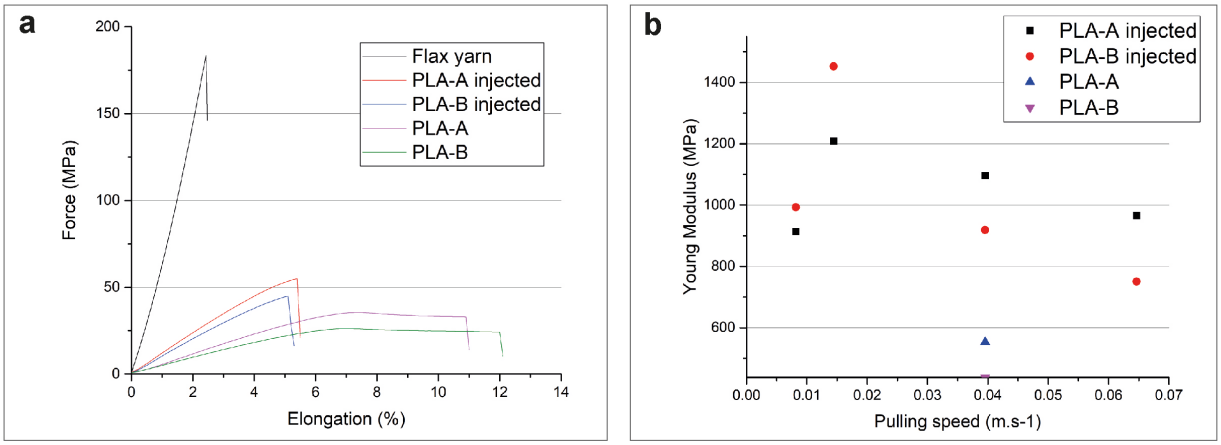

Fig. 7. Stress strain curve (a) and Young's modulus (b) of flax yarn, PLA coated flax and pure PLA filaments.

Summary

In the present work, a wire-coating die was used to manufacture novel filament of flax yarn with a PLA coating. The material properties were assessed to check whether the polymer properties are suitable with the extrusion process.

The main conclusions of this research work are as follows:

- The two grades of PLA are suitable to be extruded in a wire-coating die. A range of filaments with various diameters was successfully achieved.
- The filament diameter decreases when the pulling speed increases
- The tensile properties of the PLA coated flax and better than pure PLA filaments.

This work demonstrates the ability to obtain flax/PLA filaments. Further work will focus on printing composite parts with such filaments. Also, it might be relevant to study the interfacial adhesion between the flax yarn and the PLA matrix to enhance the mechanical properties of the composites obtained by 3D printing.

References

[1] J.J. Andrew, H.N. Dhakal, Sustainable biobased composites for advanced applications: recent trends and future opportunities – A critical review, Compos. Part C: Open Access 7 (2022) 100220. https://doi.org/10.1016/j.jcomc.2021.100220

[2] T. Gurunathan, S. Mohanty, S.K. Nayak, A review of the recent developments in biocomposites based on natural fibres and their application perspectives, Compos. Part A: Appl. Sci. Manuf. 77 (2015) 1-25. https://doi.org/10.1016/j.compositesa.2015.06.007

[3] M.P.M. Dicker, P.F. Duckworth, A.B. Baker, G. Francois, M.K. Hazzard, P.M. Weaver, Green composites: A review of material attributes and complementary applications, Compos. Part A: Appl. Sci. Manuf. 56 (2014) 280-289. https://doi.org/10.1016/j.compositesa.2013.10.014

[4] O. Faruk, A. K. Bledzki, H.-P. Fink, M. Sain, Biocomposites reinforced with natural fibers: 2000–2010, Prog. in Polym. Scie. 37 (2012) 1552-1596.

[5] A.N. Netravali, S. Chabba, Composites get greener, Mat. Today 6 (2003) 22-29. https://doi.org/10.1016/S1369-7021(03)00427-9

[6] L. Pil, F. Bensadoun, J. Pariset, I. Verpoest, Why are designers fascinated by flax and hemp fibre composites?, Compos. Part A: Appl. Sci. Manuf. 83 (2016) 193-205. https://doi.org/10.1016/j.compositesa.2015.11.004

[7] A. Melelli, O. Arnould, J. Beaugrand, A. Bourmaud, The Middle Lamella of Plant Fibers Used as Composite Reinforcement: Investigation by Atomic Force Microscopy, Molecules 25 (2020) 632. https://doi.org/10.3390/molecules25030632

[8] C. Baley, F. Busnel, Y. Grohens, O. Sire, Influence of chemical treatments on surface properties and adhesion of flax fibre–polyester resin, Compos. Part A: Appl. Sci. Manuf. 37 (2006) 1626-1637. https://doi.org/10.1016/j.compositesa.2005.10.014

[9] D. Stoof, K. Pickering, Y. Zhang, Fused Deposition Modelling of Natural Fibre/Polylactic Acid Composites, J. Compos. Sci. 1 (2017) 8. https://doi.org/10.3390/jcs1010008

[10] S. Valvez, P. Santos, J.M. Parente, M.P. Silva, P.N.B. Reis, 3D printed continuous carbon fiber reinforced PLA composites: A short review, Procedia Struct. Integrity 25 (2020) 394-399. https://doi.org/10.1016/j.prostr.2020.04.056

[11] G. Rajeshkumar, S. Arvindh Seshadri, G.L. Devnani, M.R. Sanjay, Suchart Siengchin, J. Prakash Maran, Naif Abdullah Al-Dhabi, Ponmurugan Karuppiah, Valan Arasu Mariadhas, N. Sivarajasekar, A. Ronaldo Anuf, Environment friendly, renewable and sustainable poly lactic acid (PLA) based natural fiber reinforced composites – A comprehensive review, J. Clean. Prod. 310 (2021) 127483. https://doi.org/10.1016/j.jclepro.2021.127483

[12] AFNOR, NF EN ISO 2062 - Textiles - Yarns from packages - Determination of single-end breaking force and elongation at break using constant rate of extension (CRE) tester, 2010

[13] D. Garlotta, A Literature Review of Poly(Lactic Acid), Jour. of Poly. and the Envi. 9 (2001) 63-84. https://doi.org/10.1023/A:1020200822435

[14] J. Huang, M.S. Lisowski, J. Runt, E.S. Hall, R.T. Kean, N. Buehler, J.S. Lin, Crystallization and Microstructure of Poly(L -lactide- *co* - *meso* -lactide) Copolymers, Macromolecules 31(1998) 2593-2599. https://doi.org/10.1021/ma9714629
[15] G.L. Siparsky, K.J. Voorhees, J.R. Dorgan, K. Schilling, Water transport in polylactic acid (PLA), PLA/ polycaprolactone copolymers, and PLA/polyethylene glycol blends, Jour. of Envir. Polym. Degrad. 5 (1997) 125-136. https://doi.org/10.1007/BF02763656
[16] G. Perego, G.D. Cella, C. Bastioli, Effect of molecular weight and crystallinity on poly(lactic acid) mechanical properties, J. Appl. Polym. Sci. 59 (1996) 37-43. https://doi.org/10.1002/(SICI)1097-4628(19960103)59:1<37::AID-APP6>3.0.CO;2-N
[17] Q. Fang, M.A. Hanna, Rheological properties of amorphous and semicrystalline polylactic acid polymers, Industrial Crops and Products 10 (1999) 47-53. https://doi.org/10.1016/S0926-6690(99)00009-6
[18] Y. Ikada, K. Jamshidi, H. Tsuji, S.H. Hyon, Stereocomplex formation between enantiomeric poly(lactides), Macromolecules 20 (1987) 904-906. https://doi.org/10.1021/ma00170a034
[19] S. Saeidlou, M.A. Huneault, H. Li, P. Sammut, C.B. Park, Evidence of a dual network/spherulitic crystalline morphology in PLA stereocomplexes, Polymer 53 (2012) 5816-5824. https://doi.org/10.1016/j.polymer.2012.10.030
[20] H. J. Lehermeier, J.R. Dorgan, Melt rheology of poly(lactic acid): Consequences of blending chain architectures, Polym. Eng. Sci. 41 (2001) 2172-2184. https://doi.org/10.1002/pen.10912
[21] N. El Kissi, J.-M. Piau, F. Toussaint, Sharkskin and cracking of polymer melt extrudates, J. Non-Newtonian Fluid Mech. 68 (1997) 271-290. https://doi.org/10.1016/S0377-0257(96)01507-8